

Mechanical characterisation of wall tie connection in cavity walls

Skroumpelou, Georgia; Messali, Francesco; Esposito, Rita; Rots, Jan

Publication date

2018

Document Version

Accepted author manuscript

Published in

10th Australasian Masonry Conference

Citation (APA)

Skroumpelou, G., Messali, F., Esposito, R., & Rots, J. (2018). Mechanical characterisation of wall tie connection in cavity walls. In *10th Australasian Masonry Conference: 11 - 14 February, 2018, Sydney, Australia*

Important note

To cite this publication, please use the final published version (if applicable). Please check the document version above.

Copyright

Other than for strictly personal use, it is not permitted to download, forward or distribute the text or part of it, without the consent of the author(s) and/or copyright holder(s), unless the work is under an open content license such as Creative Commons.

Takedown policy

Please contact us and provide details if you believe this document breaches copyrights. We will remove access to the work immediately and investigate your claim.

MECHANICAL CHARACTERIZATION OF WALL TIE CONNECTION IN CAVITY WALLS

G. Skroumpelou¹, F. Messali², R. Esposito³ and J.G. Rots⁴

¹ Graduate student, Delft University of Technology, Section of Structural Mechanics, Delft, ZH, The Netherlands, G.Skroumpelou@student.tudelft.nl

² Postdoctoral researcher, Delft University of Technology, Section of Structural Mechanics, Delft, ZH, The Netherlands, F.Messali@tudelft.nl

³ Postdoctoral researcher, Delft University of Technology, Section of Structural Mechanics, Delft, ZH, The Netherlands, R.Esposito@tudelft.nl

⁴ Full professor, Delft University of Technology, Section of Structural Mechanics, Delft, ZH, The Netherlands, J.G.Rots@tudelft.nl

The assessment of the seismic response of unreinforced masonry (URM) buildings has been a popular topic all over the world in the last decades. In recent years, induced seismicity in the north of the Netherlands increased considerably and introduced seismic risk also in this country. The built environment in the region is mainly composed by unreinforced masonry buildings, which are not designed for seismic loading and have specific characteristics such as the use of cavity walls.

An extensive large-scale testing program has been recently carried out at Delft University of Technology to characterize the behaviour at material and structural level of the terraced house typology, which is characterised by the presence of cavity walls with loadbearing walls of calcium silicate bricks and veneer walls of perforated clay bricks. Experimental tests showed that the wall ties are able to connect the two leaves for small loads, but they may fail for higher accelerations and increase the probability of out-of-plane collapse of the wall. In this framework, the paper reports the outcomes of an extensive testing campaign on the connections between the two leaves of cavity walls under large imposed displacements, aiming at providing a complete characterization of the behaviour of the connections in terms of resistance, envelope curve and dissipated energy. The specimens were composed by the typical wall ties employed in Dutch terraced houses, embedded either in calcium silicate brick masonry or in perforated clay brick masonry. Different loading conditions (axial and shear, monotonic and cyclic loading) and different confining compressive loads on the couplets were considered.

Keywords: Unreinforced masonry, Cavity walls, Wall ties, Quasi-static tests, Cyclic.

INTRODUCTION

In the last years, the increasing seismicity in the northern part of the Netherlands has led to extensive research on the seismic assessment of the existing structures, as well as on possible strengthening methods. Most of the built environment in the area is composed of unreinforced masonry (URM) buildings. To provide benchmarks for the Dutch situation, an extensive testing campaign was performed at Delft University of Technology in 2015 (Esposito et al, 2017; Messali et al 2017; Esposito et al, 2018). The campaign focused on terraced houses (one of the most diffuse building typologies in the Netherlands) that is characterized by the use of cavity walls, similarly to URM buildings in other regions of the world, such as Australia, New Zealand, North America, and other parts of northern Europe. A cavity wall consists of two separate parallel walls cooperating as one wall, with a space between them, which is called cavity (Figure 1a). The inner and outer walls are also called leaves of the wall and are interconnected by means of metal ties, as described in NEN-EN 845-1 (2016). In comparison with solid walls, cavity walls offer better thermal and sound insulation, they prevent ambient moisture to enter the building and they are less expensive to construct (Products, 2016).

The out-of-plane mechanisms represent the primary cause of structural failure in URM buildings under seismic loading, particularly for poor wall-to-diaphragm or wall-to-floor connections. Such failure can involve either the outer leaf or both leaves of the cavity wall, depending on the effectiveness of the connection provided by the wall ties. The ties should be placed in specific locations, spread almost uniformly over the area of the wall. The exact density and positioning of the ties vary according to different building regulations. As an indication of the distribution of the ties, BS EN 6697 (2010) suggests that, except around openings, not less than 2.5 ties per square meter (900 mm horizontal \times 450 mm centres) should be used for walls in which both leaves are 90 mm or thicker. Insufficient embedment of the tie in the mortar joint or inadequate number of ties could lead to reduction of the overall capacity of the cavity wall (Giaretton et al, 2016a).

This study aims at providing a complete description the seismic behaviour of the connections between the two wall leaves. The mechanical characterization of the connections in cavity walls can be achieved with tests at component level (Mertens et al, 2014) or for full scale structures (Walsh et al, 2015; Graziotti et al, 2016; Giaretton et al, 2016b). The latter tests showed that the connection may fail before the out-of-plane collapse of the wall.

The present study focuses on the component level. The simplest nevertheless realistic component of a URM wall consists of a couple of bricks connected by means of mortar, including an embedded wall tie. This component will be referred to as “the couplet” from this point onwards. The application of constant precompression will compensate for the absence of the surrounding wall. Assuming that one of the leaves is fixed, the relative motion of the free leaf can occur in three directions: two directions are parallel to the plane of the fixed leaf (vertical and horizontal shear loading) and one is perpendicular (axial loading) (Figure 1b). In the case of the couplets, the clamp will replace the free leaf. The testing setup allows only the application of vertical displacement. Therefore, the orientation of the couplets was adjusted accordingly to simulate the aforementioned relative displacements. At this point it should be noted that, in the framework of this research, the case of vertical shear loading was not tested, as the flexural failure of the tie would most probably be the governing failure mechanism. Besides, in real walls the ties are often

slightly bent to connect mortar layers at different height. This actual configuration has not been considered in the current testing campaign, and only straight ties have been tested.

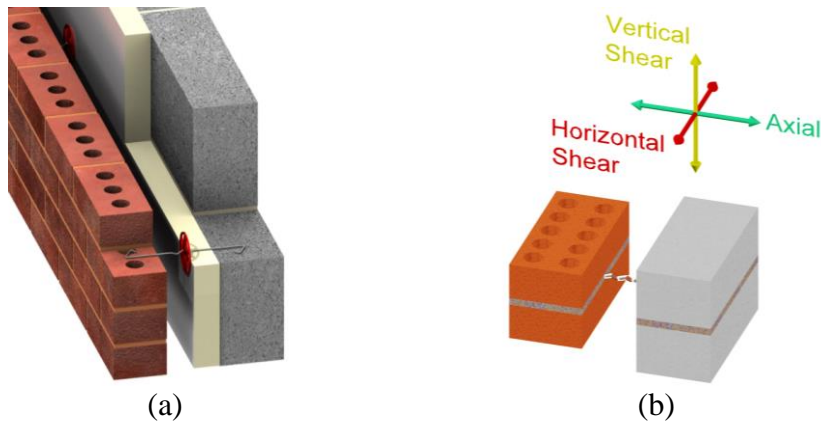


Figure 1: Cavity wall (a) and relative motions between wall leaves (b)

MATERIALS AND METHODS

Asymmetrical L-shaped ties with a diameter of 3.6 mm and a length of 200 mm are used. One end of the wall ties is hooked and the other one is zig-zagged. The couplets representative of the inner and outer leaves are composed of calcium silicate CS (102×212×71 mm) and perforated clay bricks (100×210×50 mm), respectively, and general purpose mortar. The cavity is 80 mm wide.

As components of the cavity walls, two types of couplets are investigated:

- CS specimens: the hooked part of the tie is embedded in a calcium silicate masonry couplet, with an anchoring length of 70 mm (Figure 2a).
- Clay specimens: the zig-zagged part of the tie is embedded in a clay masonry couplet with an anchoring length of 50 mm (Figure 2b).

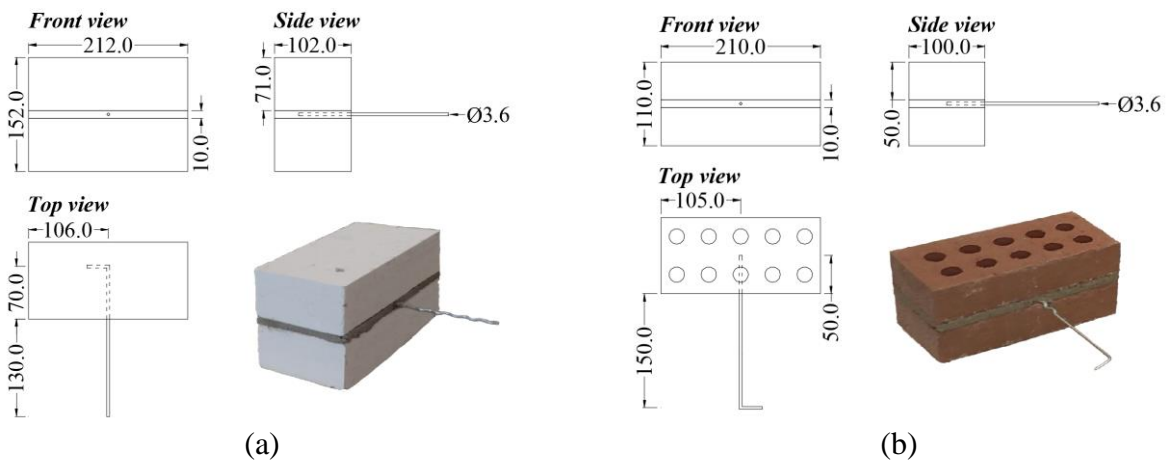


Figure 2: Couplets: CS specimens (a); Clay specimens (b)

The general testing setup for both the axial and shear tests was based on the recommendations reported in EN 846-5 (2012) and EN-846-7 (2012) and is presented in Figure 3a. It comprises:

- A horizontal steel plate, connected to a lower horizontal beam by means of steel threaded rods, to prevent the vertical displacements of the specimen. The specimen is supported by hardwood bearers that do not apply any restraint against splitting of the specimen.
- An apparatus to apply and maintain constant the lateral compressive stresses on the couplet. The force is provided by a hydraulic jack acting in the horizontal direction and perpendicular to the bed joint plane. The system is self-equilibrated by four threaded bars connecting the two vertical steel plates; the outer plate is fixed and the inner plate can slide when pushed by the piston.
- A test machine to apply the vertical load. The load is applied in a vertical direction using a displacement controlled apparatus, with a 4.5 t jack. The machine is provided with a clamp for gripping efficiently the free end of the tie, connected to the jack by means of a bolt.

The clamp and the orientation of the specimen in the setup depend on the type of test. Regarding the axial tests, a standard clamp. The specimen is oriented in such way that the long axis of the tie is vertical and the plane of the mortar parallel to the vertical steel plates (Figure 3b). As for the shear tests, a stiff clamp of custom design was manufactured to maintain the same general configuration of the setup. The specimen was placed in the setup with the tie being horizontal and, as for the axial tests, the plane of the mortar joint being vertical and parallel to the steel plates (Figure 3c). In both cases, the distance between the face of the bricks and the clamp was 80 mm, equal to the cavity width. In Figure 3b and Figure 3c the precompression and support systems are not included for the sake of clarity.

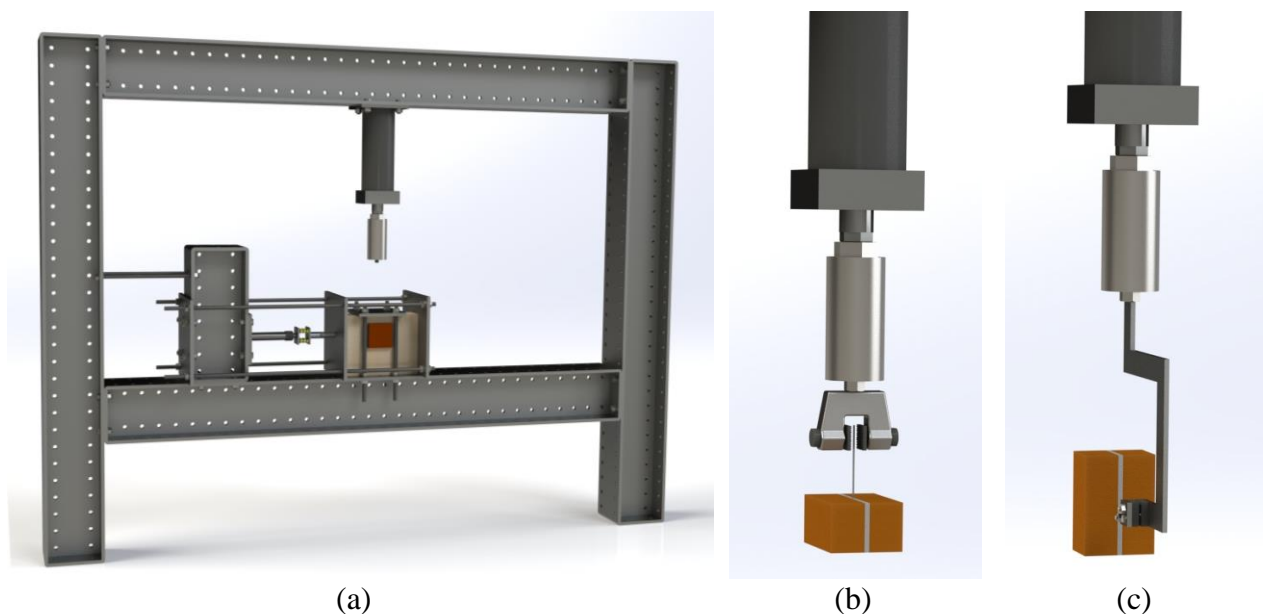


Figure 3: Testing setup: General setup (a); Axial setup (b); Shear setup (c)

Six different loading schemes are followed. The abbreviations used for naming the loading protocols are based on the following convention: A=Axial load, S=Shear load, M=Monotonic

load, **Cy**=**C**yclic load, **T**=**T**ension load, **C**=**C**ompression load. The description of each protocol is presented below.

- **Protocol A_{MT}** (monotonic tensile protocol): monotonic increase of the displacement with a rate of 0.1 mm/s up to failure.
- **Protocol A_{MC}** (monotonic compressive protocol): monotonic increase of the displacement with a rate of 0.1mm/s up to failure or up to maximum possible displacement.
- **Protocol A_{Cy}** (tensile-compressive protocol): the displacement is cyclically varied by applying both tensile and compressive loads on the tie.
- **Protocol S_M** (monotonic shear protocol): monotonic increase of the displacement with a rate of 0.1mm/s up to failure.
- **Protocol S_{Cy}** (cyclic shear protocol): the displacement is cyclically varied by applying both upward and downward (shear) loads on the tie up to failure.

All protocols are applied for two levels of precompression: $0.1 \pm 0.01 \text{ N/mm}^2$ and $0.3 \pm 0.01 \text{ N/mm}^2$. The number of tests performed according to each loading protocol for each campaign is presented in Table 1 below.

Table 1: Number of performed tests

Loading protocol	A _{MT}		A _{MC}		A _{Cy}		S _M		S _{Cy}	
	0.1	0.3	0.1	0.3	0.1	0.3	0.1	0.3	0.1	0.3
Performed tests on CS	6	13	8	8	9	6	5	5	3	3
Performed tests on clay	7	10	7	6	4	7	5	4	3	3

The loading history for the cyclic tests can be subdivided into two phases (Figure 4). In phase 1, groups of three cycles are performed, each group of increased amplitude. In phase 2, each group is composed by two cycles of increased amplitude and two cycles with reduced amplitude (40% of the first two cycles). The loading rate is such that the duration of every cycle remains constant until reaching 1 mm/s; afterwards it is maintained constant. The exact number of groups of cycles for each cyclic protocol and their amplitudes are listed in Table 2. In all of the cyclic tests, the specimen is initially loaded upwards, that is referred as the positive direction.

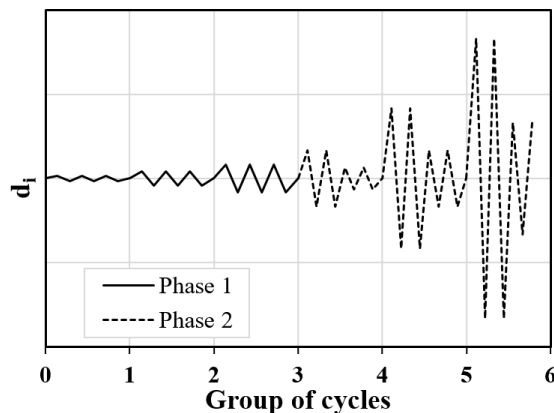


Figure 4: Cyclic protocols

Table 2: Protocols A_{Cy} and S_{Cy} – Sequence of loading

A_{Cy}	Phase	1			2												
	Group of cycles	1	2	3	4	5	6	7	8	9	10						
	Amplitude (mm)	0.1	0.25	0.5	1	0.4	2.5	1	5	2	10	4	15	6	20	8	30
S_{Cy}	Phase	1				2											
	Group of cycles	1	2	3	4	5			6			7					
	Amplitude (mm)	1	5	10	20	40	16	60	24	80	32						

TEST RESULTS

First the different failure modes obtained for the axial tests are described (Figure 5). Regarding the CS masonry couplets, failure is characterized by cracking of the bed joint and straightening of the steel tie in tension (Protocol A_{MT}) and by piercing and expulsion of the cone of mortar next to the embedded steel tie in compression (Protocol A_{MC}). For clay masonry couplets, a dowel effect is provided by the mortar in the holes, giving higher resistance in tension (Protocol A_{MT}), while the tie buckles in compression (Protocol A_{MC}). The failure mode of the specimens tested according to Protocol A_{Cy} is a combination of the mechanisms of the monotonic tests, both for CS and clay couplets.

A representative force-displacement curve is presented in Figure 6 for each type of masonry and loading procedure. The ultimate failure of the specimen is defined when 20% of the peak force is reached in the post-peak phase. The tensile and compressive curve obtained for the monotonic protocols are shown together in the same diagram. The envelope curve was derived according to ASTM-E2126-11 (2011). The qualitative behaviour of the couplets does not change for different levels of precompression, therefore only one curve is presented for each loading protocol. Figure 7 shows the peak and the ultimate failure for all loading protocols and both precompression levels for both materials, and offers a complete overview of the results. The mean peak and ultimate force/displacement, along with the standard deviation, of each sample are reported in Table 3.

By comparing the behaviour of CS and clay couplets, the clay specimens presented consistently a more brittle behaviour and higher peak load at smaller displacements. For both materials, the cyclic loading determined the failure of the specimens for lower or similar loads than the corresponding monotonic tests, except for the case of tensile loading of clay couplets at a precompression of 0.3 MPa (for which the peak load for the cyclic loading is significantly higher than that for monotonic). However, in general the influence of the lateral precompression on the peak load (and related displacement) is rather limited for the CS specimens, whereas a larger peak forces are measured for clay couplets, probably due to the increased effectiveness of the observed dowel effect.

The values of the displacement at peak vary considerably from test to test. As a general indication, for CS masonry couplets displacements of 10 mm and 2 mm for tensile and compressive loading, respectively, can be considered reasonable reference values. Smaller displacements of 3 mm and 1.5 mm for tensile and compressive loading, respectively, are measured for clay masonry couplets.

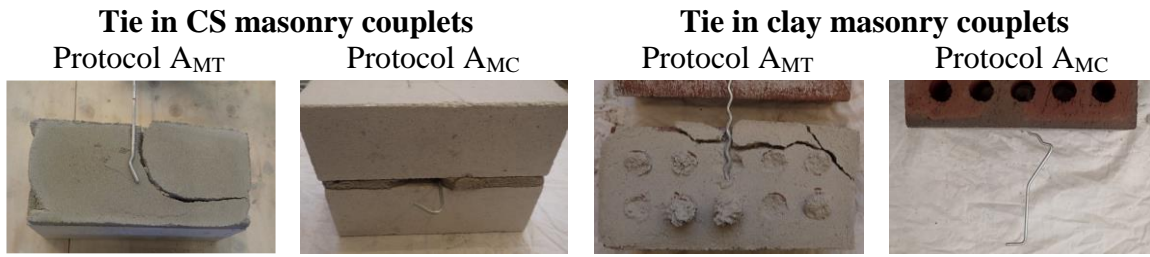


Figure 5: Failure mechanisms for Protocol A_{MT} and Protocol A_{MC} (axial loading)

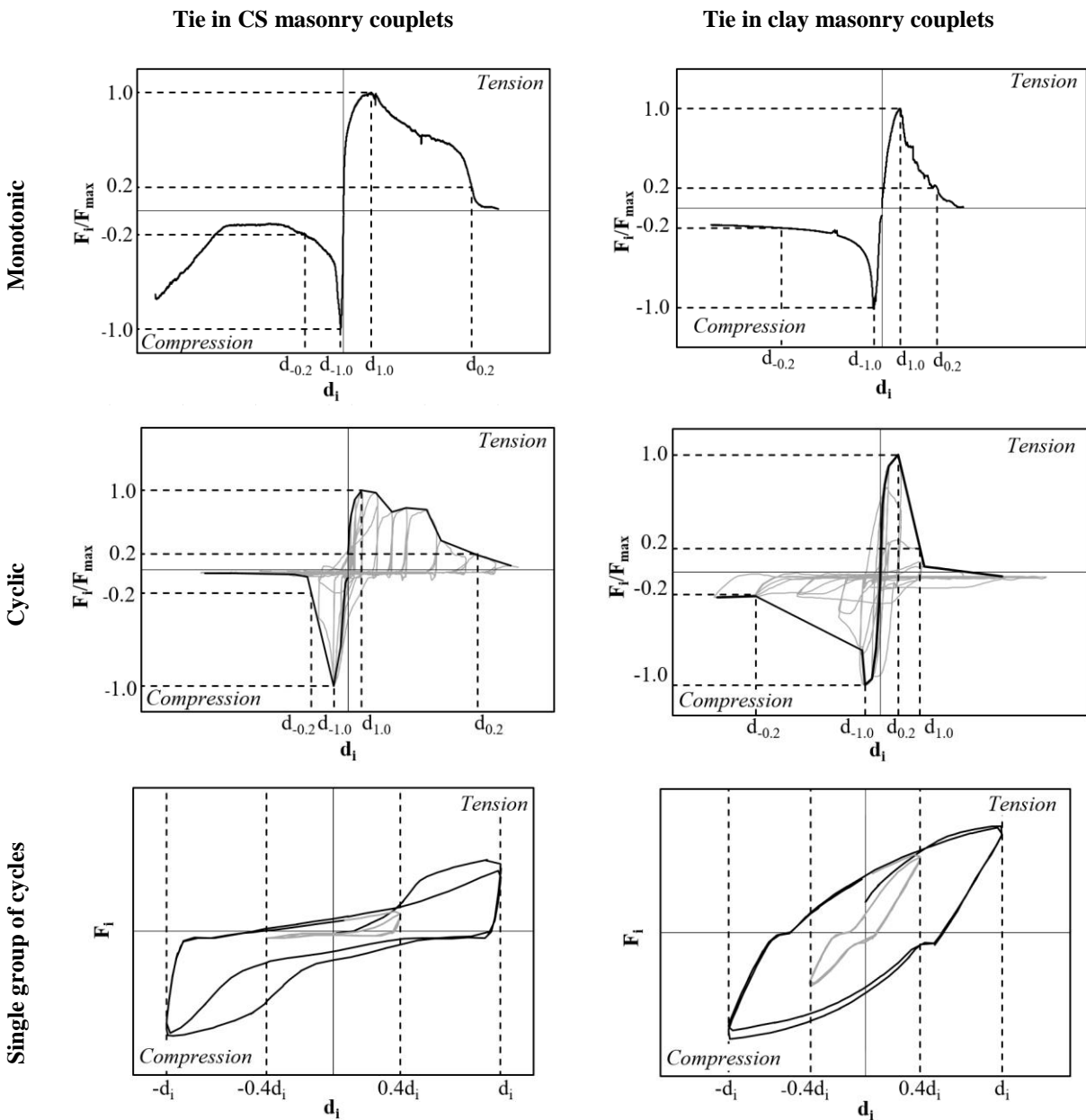


Figure 6: Indicative Force-Displacement curves for the different loading cases (axial tests)

Table 3: Results of axial tests

Type of bricks	Loading protocol	Precompression stress [MPa]	Peak force [kN]	Displacement [mm]			
				At peak force	At 20% of peak force	n_i/n_{tot}^1	
CS	A_{MT}	0.1	1.25±0.10	10.21±1.65	49.77	1/6	
		0.3	1.34±0.14	8.44±0.80	45.23±5.61	12/13	
	A_{MC}	0.1	1.13±0.20	1.99±0.71	27.19±7.30	8/8	
		0.3	1.04±0.32	1.38±1.11	30.32	1/8	
	A_{Cy}	T	0.1	1.06±0.16	5.33±1.72	48.21±4.92	5/9
			0.3	0.97±0.08	10.54±9.19	-	0/6
		C	0.1	1.05±0.30	3.41±1.05	12.02±5.43	9/9
			0.3	0.33±0.22	0.96±0.40	10.80±8.56	5/6
Clay	A_{MT}	0.1	1.94±0.33	2.00±1.51	10.02±3.36	7/7	
		0.3	2.35±0.83	3.63±2.53	13.19±5.52	10/10	
	A_{MC}	0.1	1.78±0.28	1.69±0.57	17.15±4.12	7/7	
		0.3	1.76±0.30	1.49±0.59	17.77±7.01	5/6	
	A_{Cy}	T	0.1	1.85±0.79	2.31±0.11	5.57±1.14	2/4
			0.3	3.10±0.49	6.53±2.67	19.52±2.16	2/7
		C	0.1	1.65±0.30	1.02±0.59	14.60±0.46	4/4
			0.3	1.43±0.07	0.64±0.41	14.03±4.75	7/7

¹The number of specimens that reached this value (n_i) out of the total number of tested specimens for each loading protocol (n_{tot}) is presented since not all of the tests were carried out up to the point where the force reaches the 20% of its peak value.

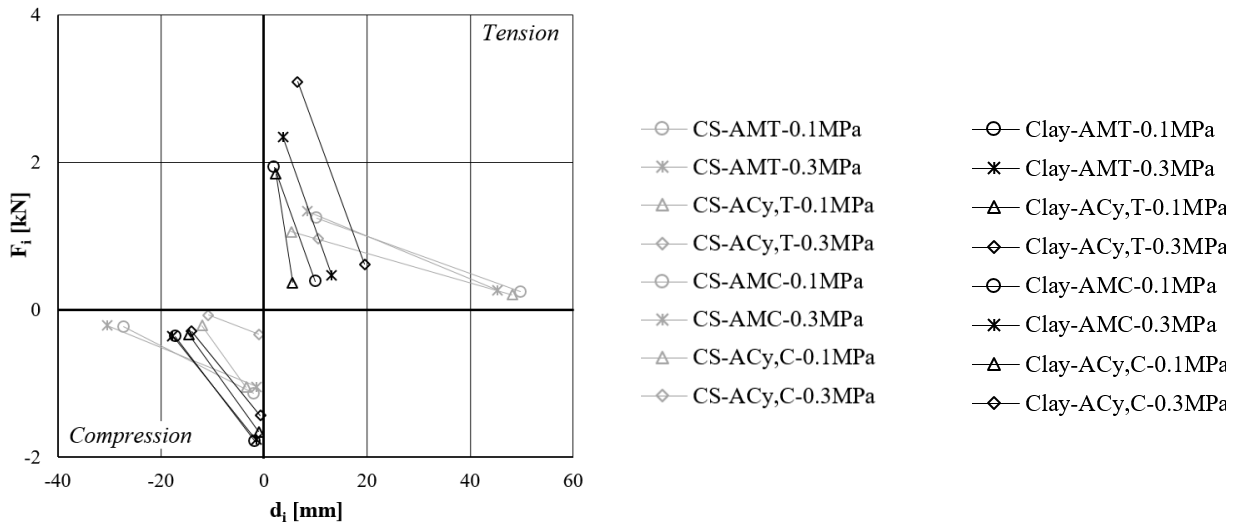


Figure 7: Peak force, 20% of peak force and corresponding displacements for the different loading cases (axial tests)

The results of the shear tests are hereinafter presented. As for the CS couplets, the observed failure mechanism for Protocol S_M was characterized by bending of the tie and often the expulsion of the cone of mortar next to the embedded steel tie. No difference was observed for

the cyclic Protocol S_{Cy} . The same failure mechanism was observed for the clay couplets for both Protocol S_M and Protocol S_{Cy} . An example of the described failure modes is shown in Figure 8.

For large displacements ($d_i \geq 20$ mm), pull-out of the ties was consistently observed, since the applied loading switched from pure shear to a combination of shear and tensile forces. This behaviour is due to the fixed horizontal distance between the clamp and the bricks, and the large imposed vertical displacements of the clamp. To avoid this coupling effect, the horizontal motion of either the specimen or the clamp should be allowed. A simple solution would be given by Teflon sheets between the specimen and the wooden supports: it may be challenging to maintain a constant precompression but the simplicity of this solution makes it noteworthy. Alternatively, the clamp may be redesigned to be free to move along the long axis of the tie. This approach is more complex but it would probably offer greater consistency of the results.

As a result of the discussed coupling effect, the shear resistance of the specimen is evaluated as the applied force for a lateral deflection of the tie of 20 mm, at which the second order effects were negligible in most of the cases. The results presented in the following figures and tables take into account this separation of loading phases. The curves on the left part of Figure 9 depict both the pure shear ($d_i < 20$ mm) and the combined ($d_i \geq 20$ mm) loading conditions. On the right part only the curves for pure shear are presented. The forces presented in Table 4 are those measured at an imposed displacement of 20 mm.

Tie in CS masonry couplets



Tie in clay masonry couplets



Figure 8: Failure mechanisms for Protocol S_M (shear loading)

Table 4: Results of shear tests

Type of bricks	Loading protocol	Precompression stress [MPa]	Shear force at displacement 20 mm [kN]	
			Upwards	Downwards
CS	S_M	0.1	0.15±0.05	
		0.3	0.09±0.01	
	S_{Cy}	0.1	0.10±0.01	0.10±0.02
		0.3	0.11±0.05	0.11±0.03
Clay	S_M	0.1	0.13±0.10	
		0.3	0.21±0.04	
	S_{Cy}	0.1	0.16±0.07	0.10±0.06
		0.3	0.11±0.02	0.12±0.01

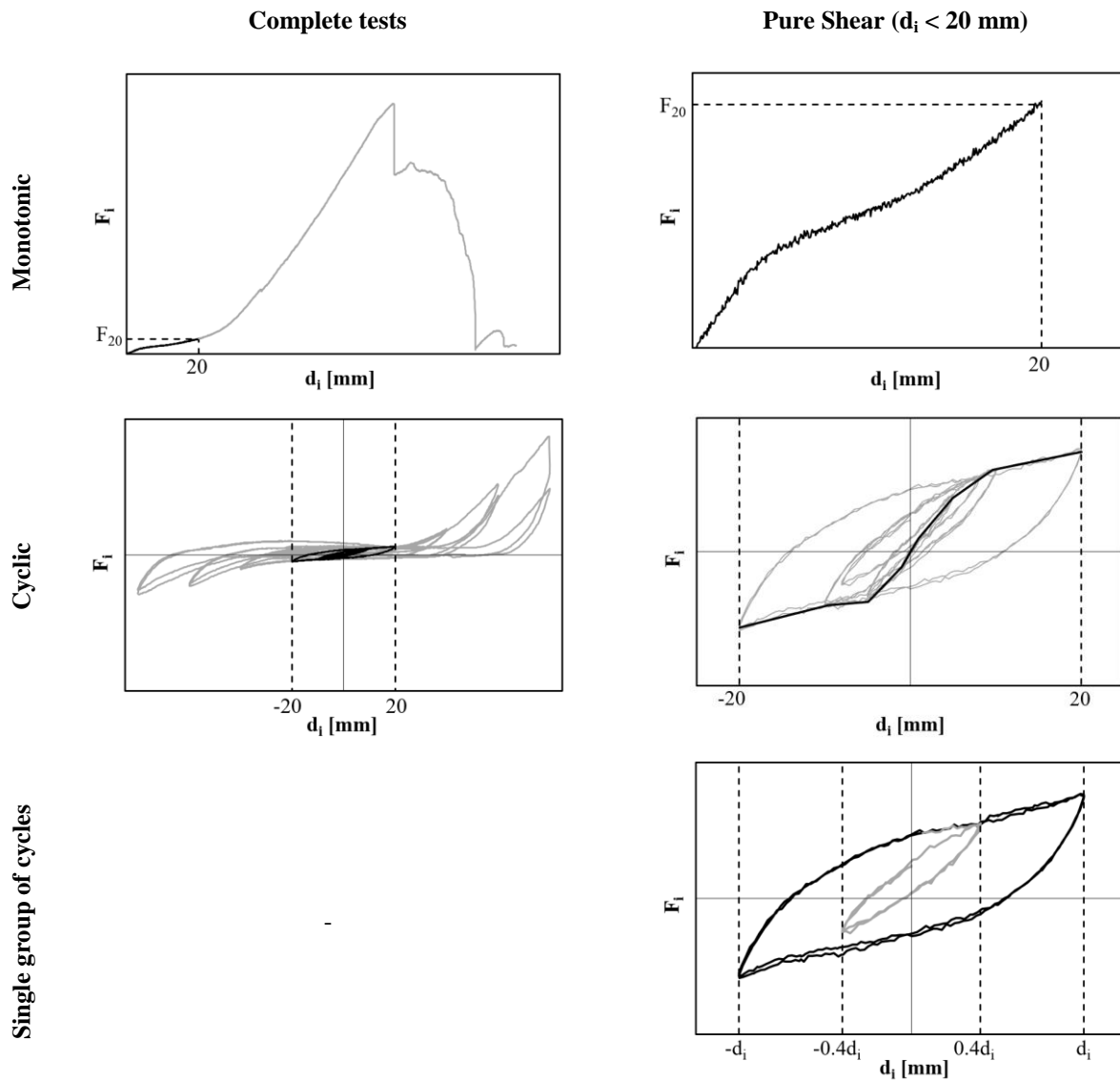


Figure 9: Indicative Force-Displacement curves for the different loading cases (shear tests) on both CS and clay specimens

The shear behaviour of the couplets (Table 4) was much more consistent than the axial (Table 3). Very similar forces were achieved at 20 mm displacement, regardless of the level of precompression and the type of loading (monotonic or cyclic), with clay couplets reaching an almost negligibly larger values. For the monotonic loading, the effect of the orientation of the embedded L-shaped end of the tie in the CS couplets was investigated. No difference was reported in the response of the two different orientations of the tie. The measured shear strength is so small that it can be easily neglected in the design of these connections, and the wall ties can be assumed able to transfer and withstand axial loading only.

CONCLUSIONS

As a part of a large-scale testing program of Delft University of Technology, this study aims at assessing the seismic response of wall tie connections in typical Dutch cavity walls.

Considering the axial tests, the clay couplets presented a more brittle behaviour and higher peak forces compared to the CS specimens. Hence, the embedment of the tie in the CS masonry would overall govern the behaviour of the connection. Cyclic loading determined a slight reduction of the peak load for both materials, while the level of precompression can be considered irrelevant to the behaviour of the connection. The compressive strength of the clay specimens, which is governed by buckling of the tie, may be lower if the tie is originally bent to connect two mortar joints at different heights, as in real walls. However, the overall connection behaviour would probably still be governed by the piercing and the expulsion of the mortar in the CS leaf, since this mechanism is significantly less resistant.

As for the shear tests, very consistent results were obtained for small displacements. The level of precompression did not affect the response of the specimens and the cyclic loading led to results similar to the monotonic. No significant difference was observed between the behaviour of the CS and clay couplets. The outcomes for large imposed displacements were affected by the coupling of axial and shear loading, a factor that should be taken into account for further testing; therefore, a new testing configuration for future campaigns should be considered.

The aforementioned results and conclusions are a first step towards the full comprehension of the seismic behaviour of connections in URM cavity walls, with specific focus to a building typology popular in the Northern part of the Netherlands.

ACKNOWLEDGEMENTS

A major part of this research was funded by NAM under contract numbers UI46268 “Physical testing and modelling – Masonry structures Groningen” and UI63654 “Testing program 2016 for Structural Upgrading of URM Structures”, which is gratefully acknowledged.

The authors are also grateful to master student Matteo Maragna for his assistance in carrying out the experimental work.

REFERENCES

BS EN 6697 (2010), Recommendations for the design of masonry structures to BS EN 1996-1-1 and BS EN 1996-2.

Esposito R., Terwel K.C., Ravenshorst G.J.P., Schipper H.R., Messali F., and Rots J.G. (2017), Cyclic pushover test on an unreinforced masonry structure resembling a typical Dutch terraced house. *Proceedings of 16th World Conference on Earthquake*, January 9-13, Santiago, Chile.

Esposito R., Safari S., Ravenshorst G.J.P., and Rots, J.G. (2018), Characterisation of calcium silicate brick and element masonry structures. *Proceedings of 10th Australasian Masonry Conference*, February 11-14, Sydney, Australia

Giaretton M., Dizhur D., Da Porto F., and Ingham J.M. (2016a), Construction details and observed earthquake performance of unreinforced clay brick masonry cavity-walls, *Structures*, Vol. 6, pp. 159-169

Giaretton M., Dizhur D., and Ingham J.M. (2016b), Shaking table testing of as-built and retrofitted clay brick URM cavity-walls, *Engineering Structures*, 125, pp. 70-79

Graziotti F., Tomassetti U., Penna A., and Magenes G. (2016), Out-of-plane shaking table tests on URM single leaf and cavity walls, *Engineering Structures*, vol. 125, pp. 455-470

Mertens S., Smits A., and Grégoire Y. (2014), Experimental parametric study on the performance of wall ties. *Proceedings of 9th International Masonry Conference*, July 7-9, Guimarães, Portugal

Messali F., Ravenshorst G., Esposito R. and Rots J.G. (2017), Large-scale testing program for the seismic characterization of Dutch masonry structures. *Proceedings of 16th World Conference on Earthquake*, January 9-13, Santiago, Chile.

NEN-EN 845-1 (2016), Specification for ancillary components for masonry - Part 1: Wall ties, tension straps, hangers and brackets, Nederlands Normalisatie-instituut (NEN).

NEN-EN 846-5 (2012), Methods of test for ancillary components for masonry - Part 5: Determination of tensile and compressive load capacity and load displacement characteristics of wall ties (couplet test), Nederlands Normalisatie-instituut (NEN).

NEN-EN 846-7 (2012), Methods of test for ancillary components for masonry - Part 7: Determination of shear load capacity and load displacement characteristics of shear ties and slip ties (couplet test for mortar joint connections), Nederlands Normalisatie-instituut (NEN).

Products, A.B. (2016), "Wall Ties & Restraint Fixings for the Construction Industry," ed, 2016.

Standard A.S.T.M. E2126-11 (2011), Standard Test Methods for Cyclic (Reversed) Load Test for Shear Resistance of Vertical Elements of the Lateral Force Resisting Systems for Buildings," ASTM International, West Conshohocken, PA.

Walsh K.Q., Dizhur D.Y., Shafaei J., Derakhshan H., and Ingham J.M. (2015), In situ out-of-plane testing of unreinforced masonry cavity walls in as-built and improved conditions. *Structures*, Vol. 3, pp. 187-199